Current Status of DMICA: exploring Dark Matter in natural muscovite MICA

Shigenobu Hirose

MDvDM 2025

Japan Agency for Marine-Earth Science and Technology (JAMSTEC)

Collaboration with:
Natsue Abe[1] Qing Chang[1], Takeshi Hanyu[1], Noriko Hasebe[2], Yasushi Hoshino[3], Takashi Kamiyama[4], Yoji Kawamura[1], Kohta Murase[5], Tatsuhiro Naka[6], Kenji Oguni[1], Katsuhiko Suzuki[1], Seiko Yamasaki[7]
(JAMSTEC[1], Kanazawa U[2], Kanagawa U[3], Hokkaido U[4], Penn State[5], Toho U[6], AIST[7])

1. DMICA Overview
2. Optical profiling of Etch-pits
3. Etch-pit formation model

1. Overview of DMICA

Target material: muscovite mica $KAl_3Si_3O_{10}(OH)_2$

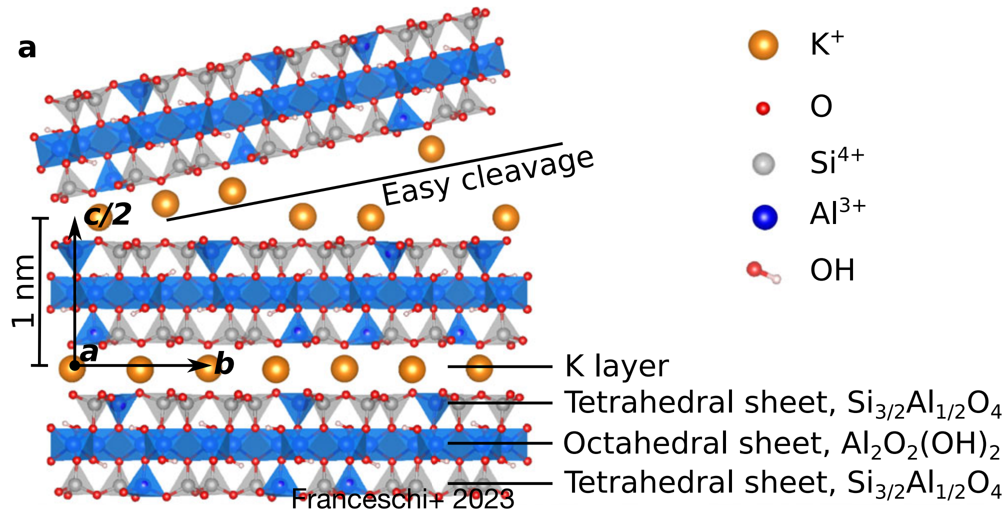

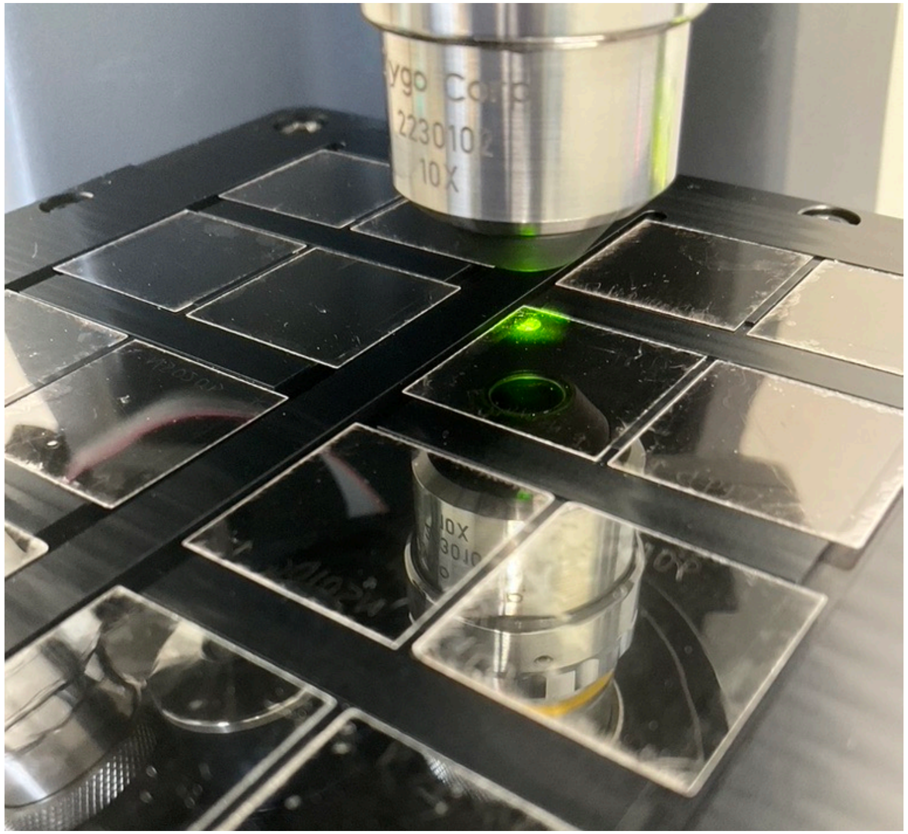

Cleaving along a potassium layer produces atomically flat, nearly perfect surfaces.

cleaved and etched mica samples under an optical profiler

Pioneering DM search with mica by Snowden-Ifft et al. 1995

VOLUME 74, NUMBER 21 PHYSICAL REVIEW LETTERS 22 MAY 1995

Limits on Dark Matter Using Ancient Mica

D. P. Snowden-Ifft,* E. S. Freeman, and P. B. Price*
Physics Department, University of California at Berkeley, Berkeley, California 94720
(Received 20 September 1994)

The combination of the track etching method and atomic force microscopy allows us to search for weakly interacting massive particles (WIMPs) in our Galaxy. A survey of 80 720 μm^2 of 0.5 Gyr old muscovite mica found no evidence of WIMP-recoil tracks. This enables us to set limits on WIMPs which are about an order of magnitude weaker than the best spin-dependent WIMP limits. Unlike other detectors, however, the mica method is, at present, not background limited. We argue that a background may not appear until we have pushed our current limits down by several orders of magnitude.

PACS numbers: 95.35.+d, 14.80.Ly, 29.40.Ym, 61.72.Ff

- Using only 0.08 mm^2 of 0.5 Gyr-old mica, they set one of the tightest WIMP cross-section limits of the time—an exposure of 10^{-6} ton · year.
- DMICA will enlarge the scanned area by six orders of magnitude, targeting 1 ton · year of exposure, by replacing AFM with an optical profiler for mica scan.

DM scattering recorded as nuclear recoil tracks

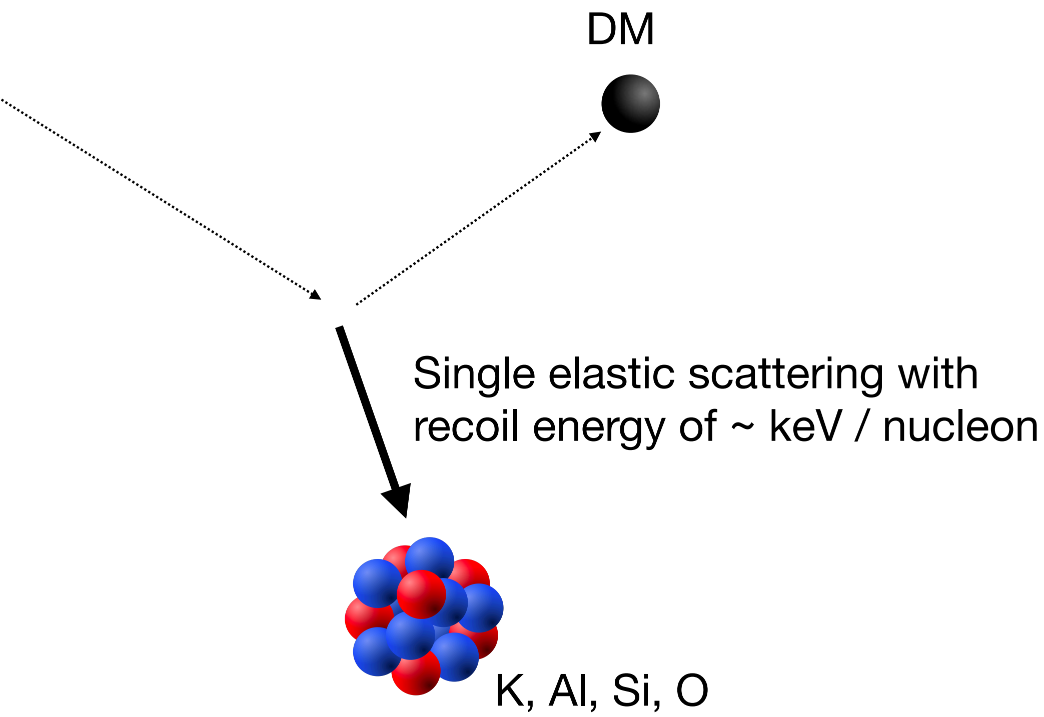

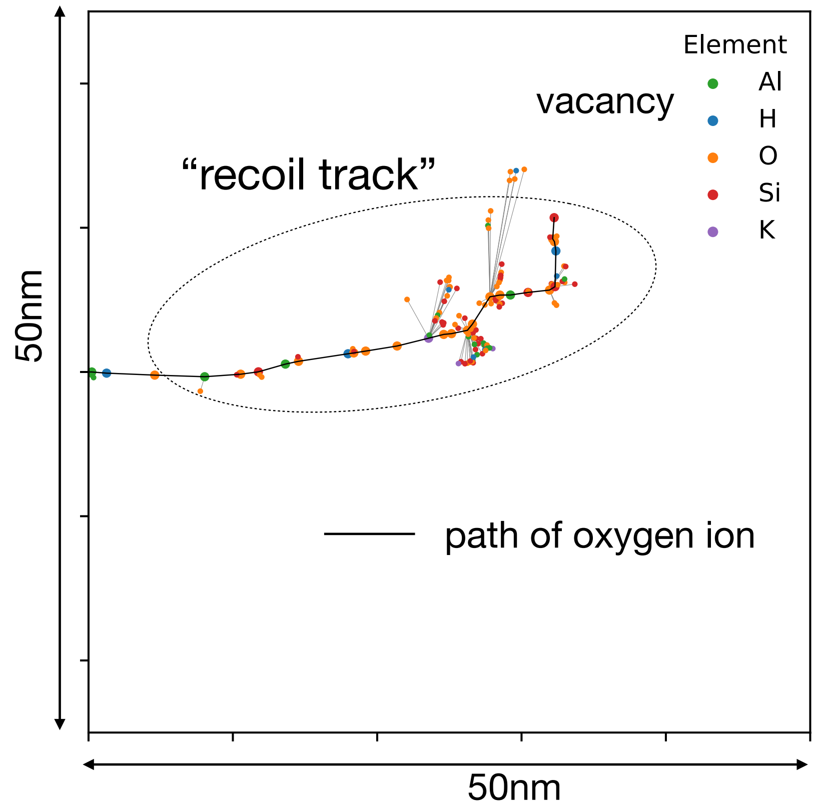

- A TRIM simulation shows a 10 keV O ion stochastically leaving atomic vacancies—its recoil track.
- Mica can retain nuclear recoil "tracks" for billions of years unless thermally annealed.

Etch-Pit Observation of Recoil Tracks

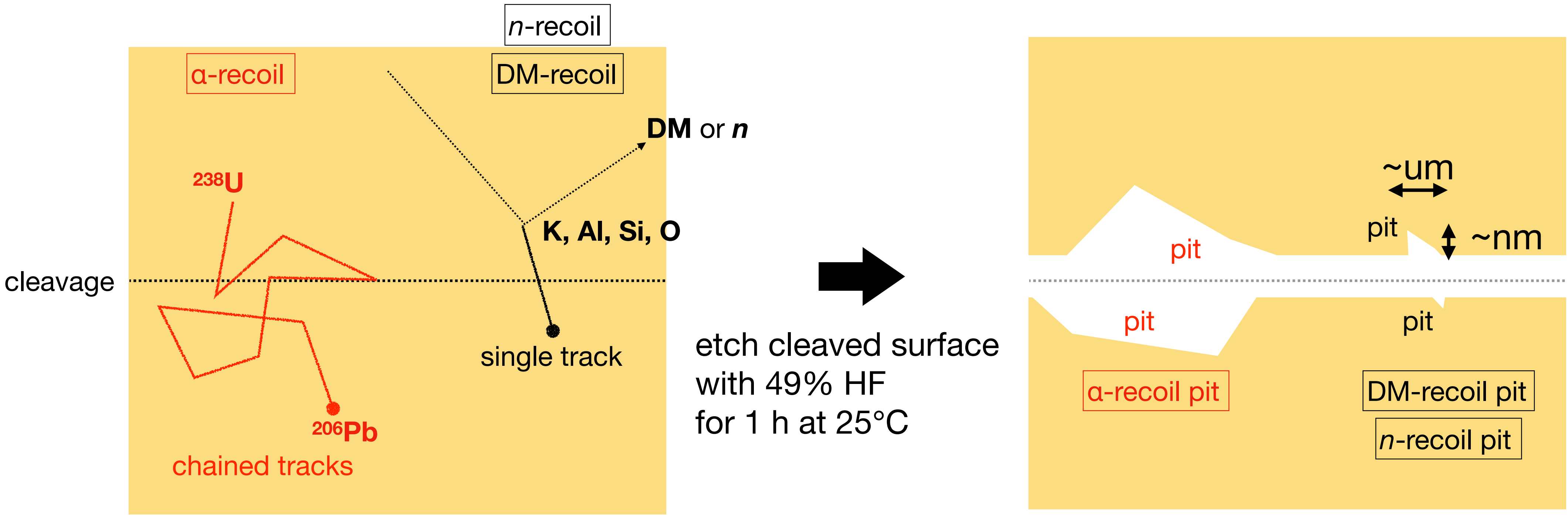

- Recoil tracks intersecting the cleavage are revealed as μm-wide, nm-deep pits after HF etching.
- Pit depth is a key observable for distinguishing DM-recoil pits from α-recoil pits.
- Fast neutron recoil pits are genuine backgrounds, being indistinguishable from DM-recoil pits.

α-recoil and neutron-recoil pits (optical profiler images)

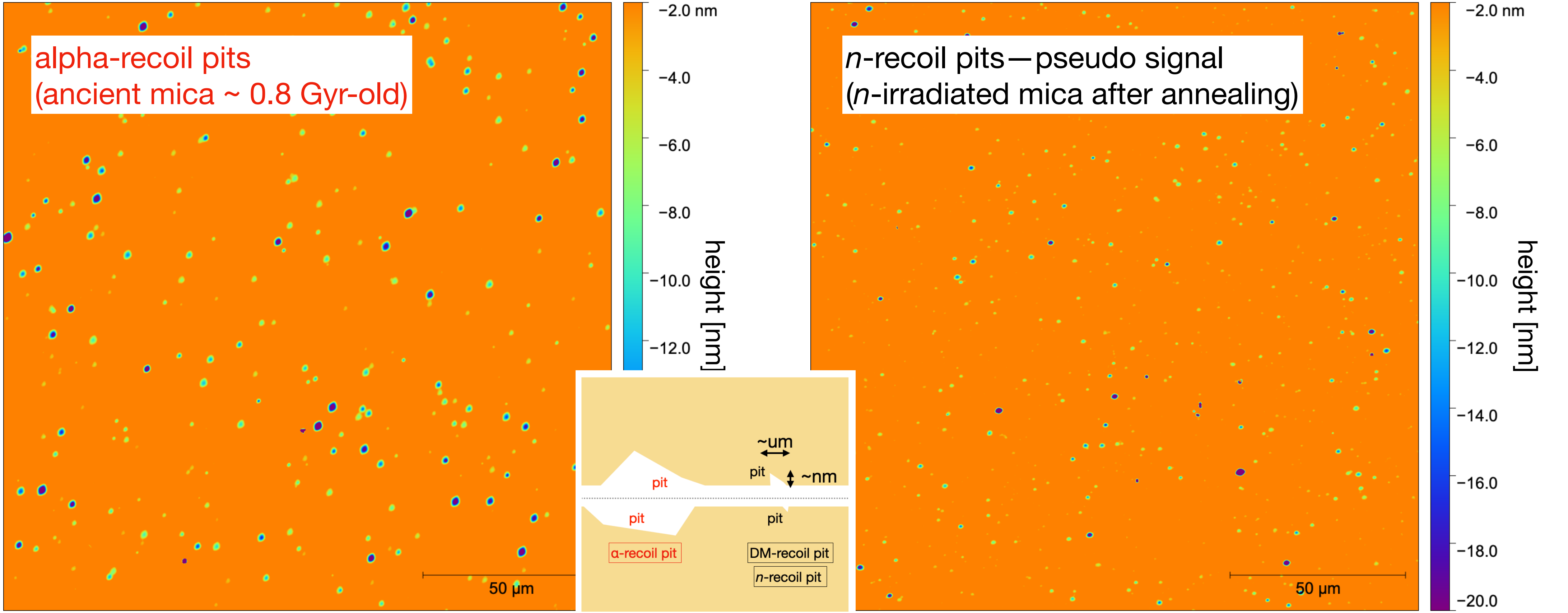

- Fast-neutron pits mimic DM recoils and illustrate mica's potential for DM detection.
- α-recoil pits are consistently deeper than fast-neutron-recoil pits.
- This depth contrast makes pit depth a key observable for separating DM signals from α-recoil backgrounds.

Pit-depth histogram and WIMP limit in Snowden-Ifft et al. (1995)

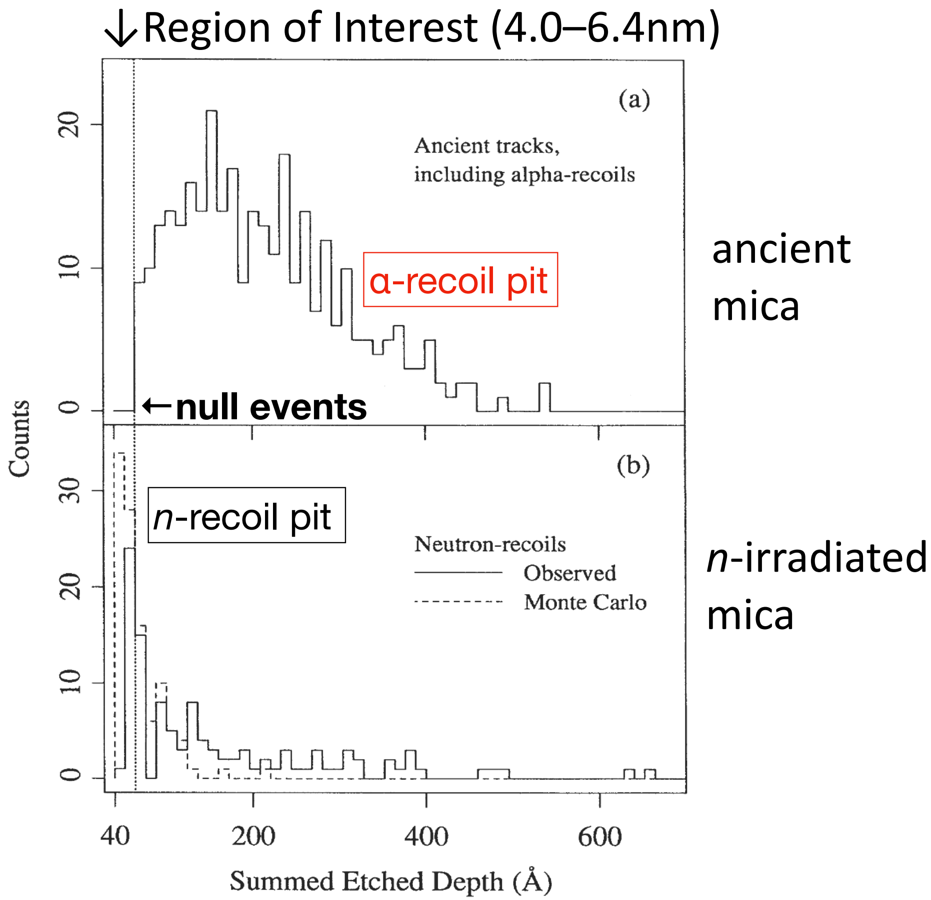

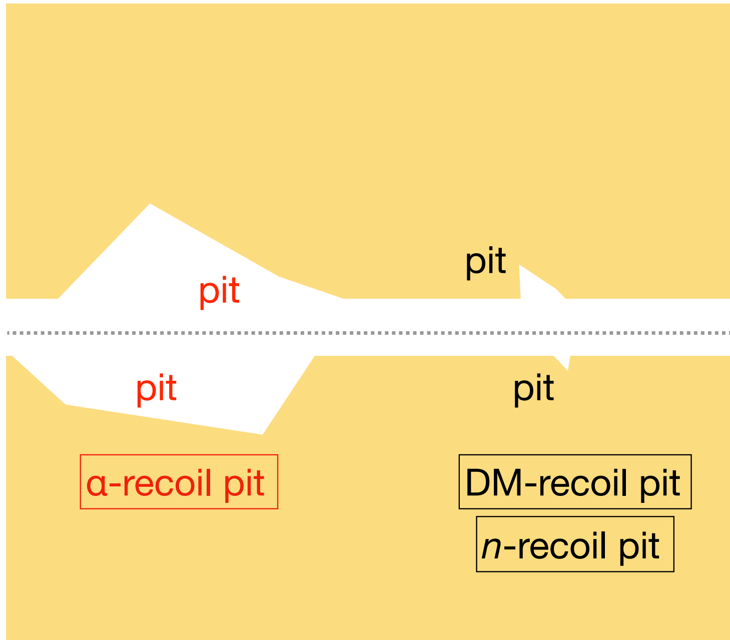

- ROI (4.0–6.4 nm) was expected to host DM pits, but no events were observed in a 0.08mm^2 mica scan.
- The null result set an upper limit on the WIMP cross section.

DMICA replaces slow AFM scanning with Fast optical profiling

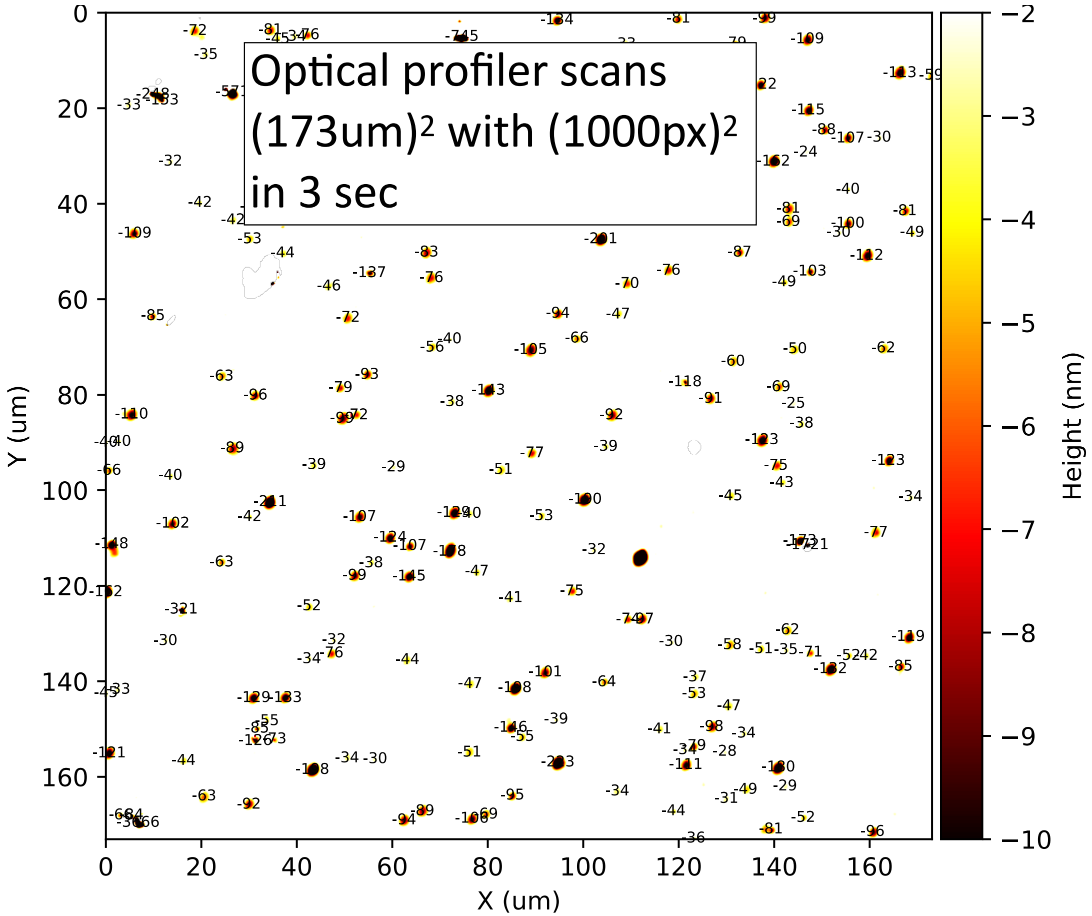

comparable
lateral resolution

AFM scans
(40um)^2 with (256px)^2
in 280 sec

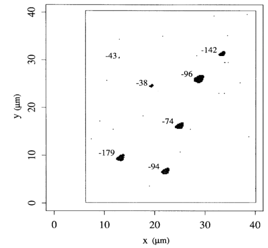

Snowden-Ifft et al. (1995)

Optical profiler covers a 173 μm × 173 μm area in 3 s, whereas AFM needed ~280 s for just 40 μm × 40 μm at similar lateral resolution.

Preliminary DMICA scan: 0.5 mm² in 53 s

DMICA: 524,765 um²
(total scan time: 53s)

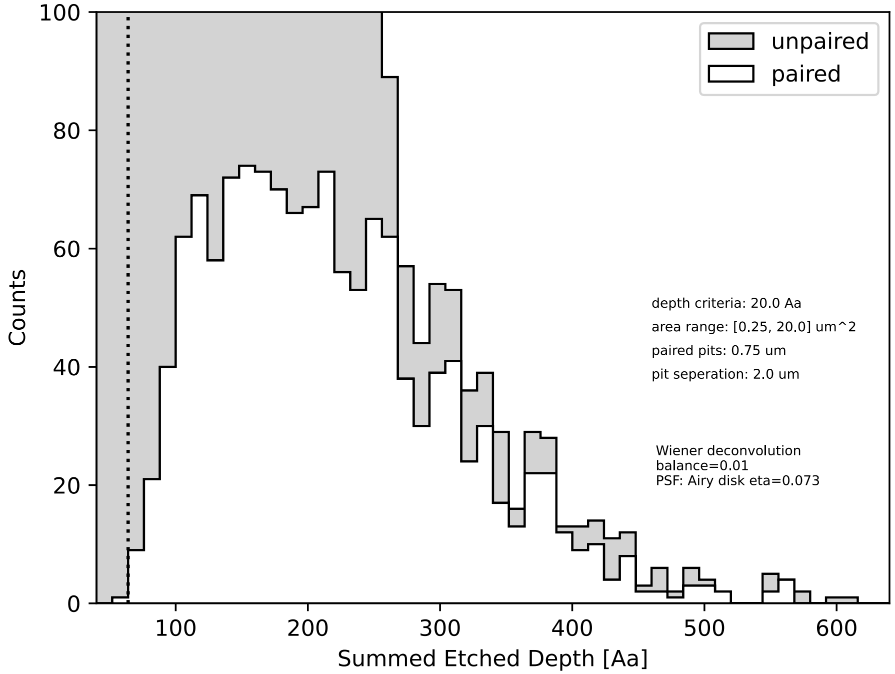

6.5x

Snowden-Ifft et al. 1995: 80,720 um²
(total scan time: 4 hrs)

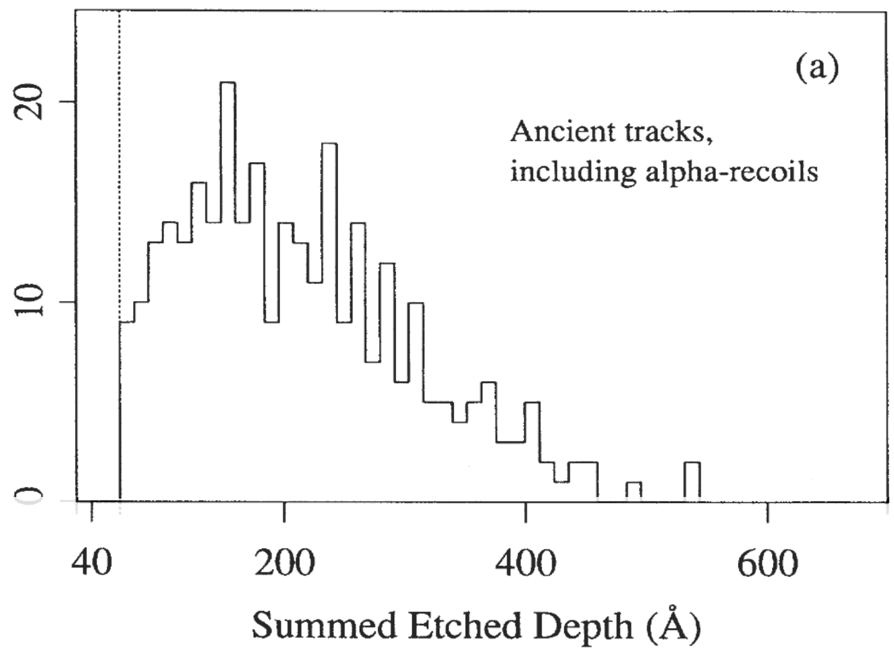

Our R&D test processed a ~0.5 mm² mica surface—about 6.5 times the area of Snowden-Ifft et al.—yet reproduced their pit-depth histogram.

Comparison of DMICA with Snowden-Ifft et al. 1995

	Snowden-Ifft et al. 1995	**DMICA**
Exposure (Scan area)	1e-6 ton-year (0.08 mm^2)	**1 ton-year** **(800 cm^2)**
Readout (Scan speed)	Atomic force microscopy (48 hr/mm^2)	**Optical profiler** **(100 sec/mm^2)**
Nominal scan time	4 hours	**92 days**
Lateral sampling	0.156 um	**0.173 um**
Backgrounds in ROI	virtually no background because of small exposure	**radiogenic fast neutrons**

By replacing slow AFM read-out with a fast optical profiler, DMICA can scale the scanned area by six orders of magnitude—reaching one ton-year of exposure—at the cost of a radiogenic fast-neutron background in the ROI.

Projected DMICA sensitivity:
1 ton-year, 0.5 Gyr integration, 800 cm² scan

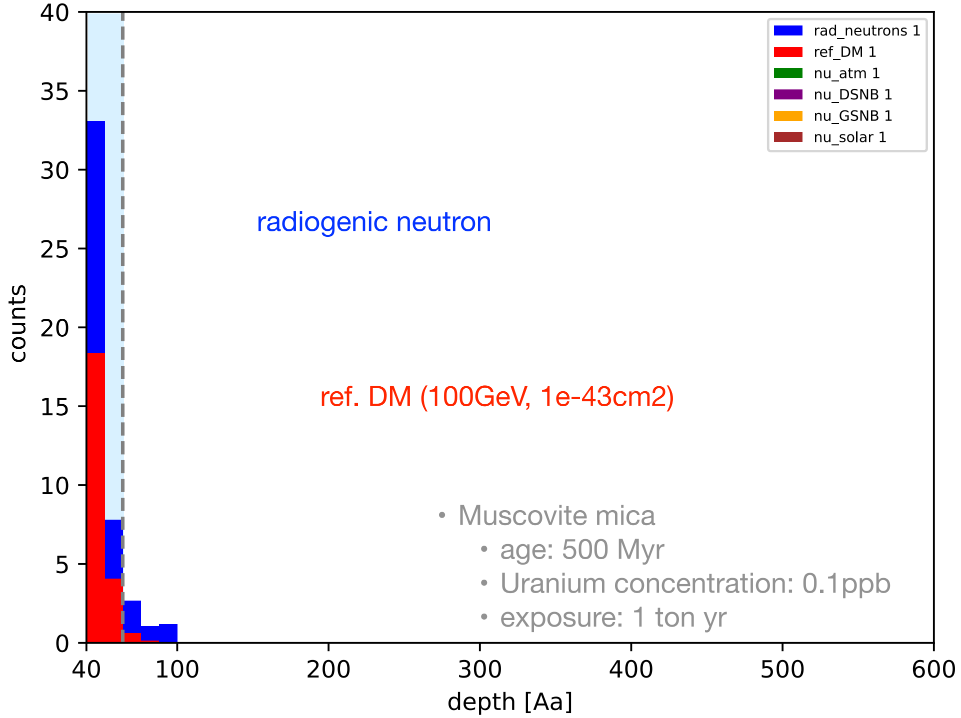

predicted pit depth histogram based on a pit-creation model
(Snowden-Ifft and Chan 1995)

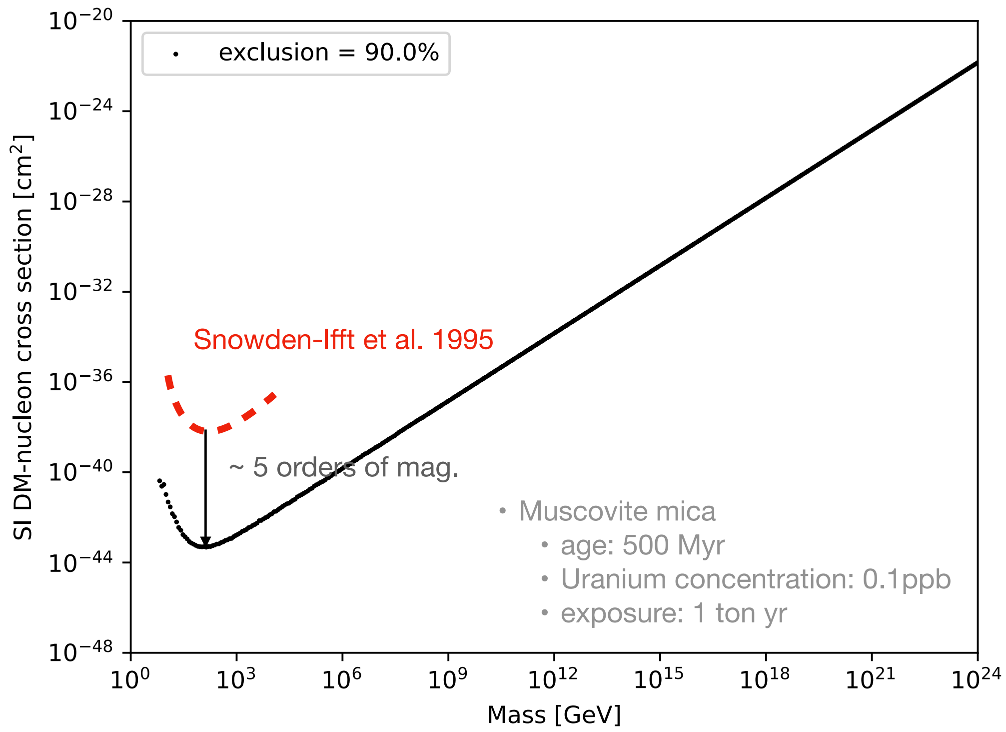

Including the radiogenic-neutron background, a 1 ton-year exposure improves the spin-independent WIMP limit by ~5 orders of magnitude relative to Snowden-Ifft et al.

Surface-to-volume advantage and 1e25 GeV mass reach

$$\text{Upper Limit on Detectable DM Mass} \propto \text{Exposure}\ (Mt) \times \text{Surface Area per Volume}\ (A/V)$$

$$\text{XENON1T:} \quad \left(\frac{m_\chi}{\text{GeV}}\right) < 10^{18} \left(\frac{Mt}{1\text{ton}\cdot\text{yr}}\right) \left(\frac{A/V}{(1\text{m})^{-1}}\right)$$

$$\text{DMICA:} \quad \left(\frac{m_\chi}{\text{GeV}}\right) < 10^{25} \left(\frac{Mt}{1\text{ton}\cdot\text{yr}}\right) \left(\frac{A/V}{(100\text{nm})^{-1}}\right)$$

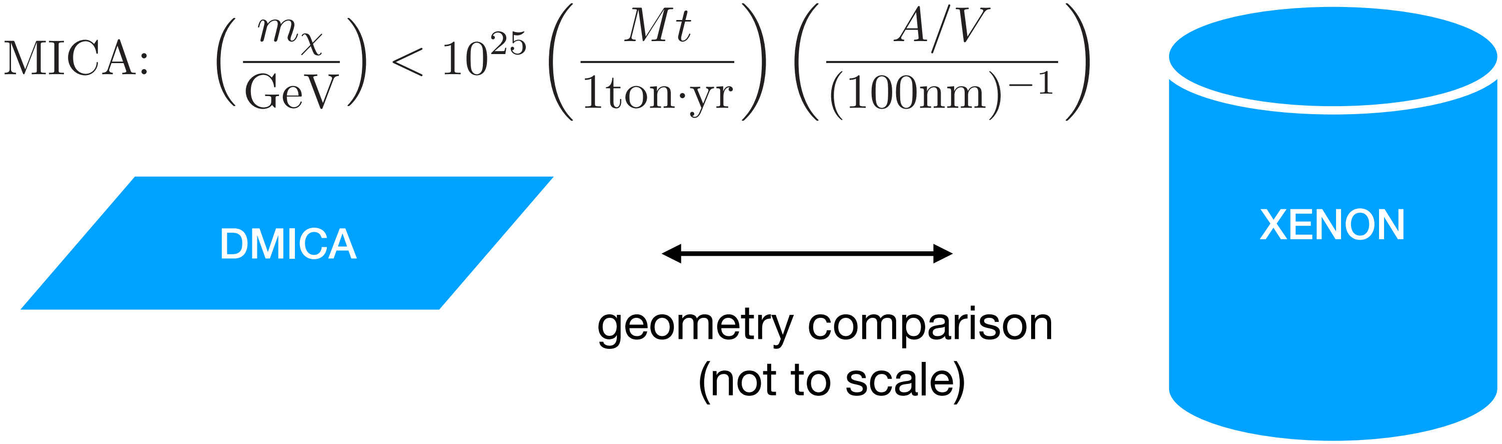

DMICA's plate geometry gives an A/V about eight orders of magnitude larger than XENON;
for the same 1 ton-year exposure, the upper limit on detectable DM mass rises to ~1e25 GeV.

Ancient minerals records Gyr-old DM events, enabling a galaxy-wide survey

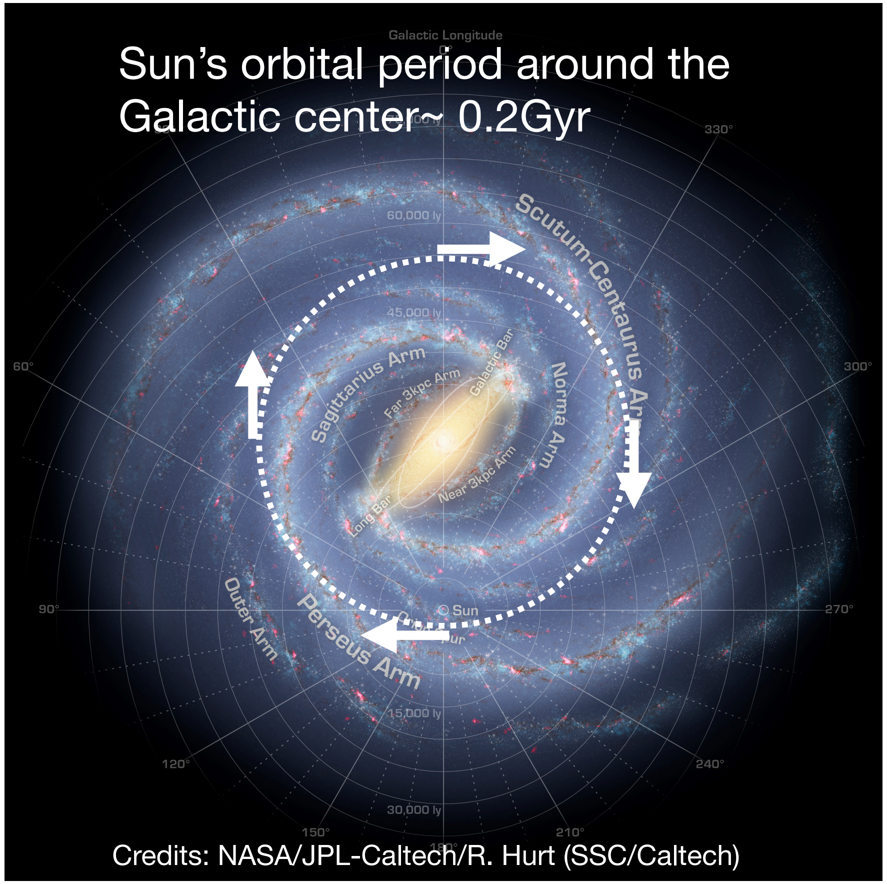

Artificial detectors capture brief, high-sensitivity snapshots, whereas minerals archive billion-year, Galaxy-wide exposure—together providing complementary insight.

2. Optical profiling of etch pits

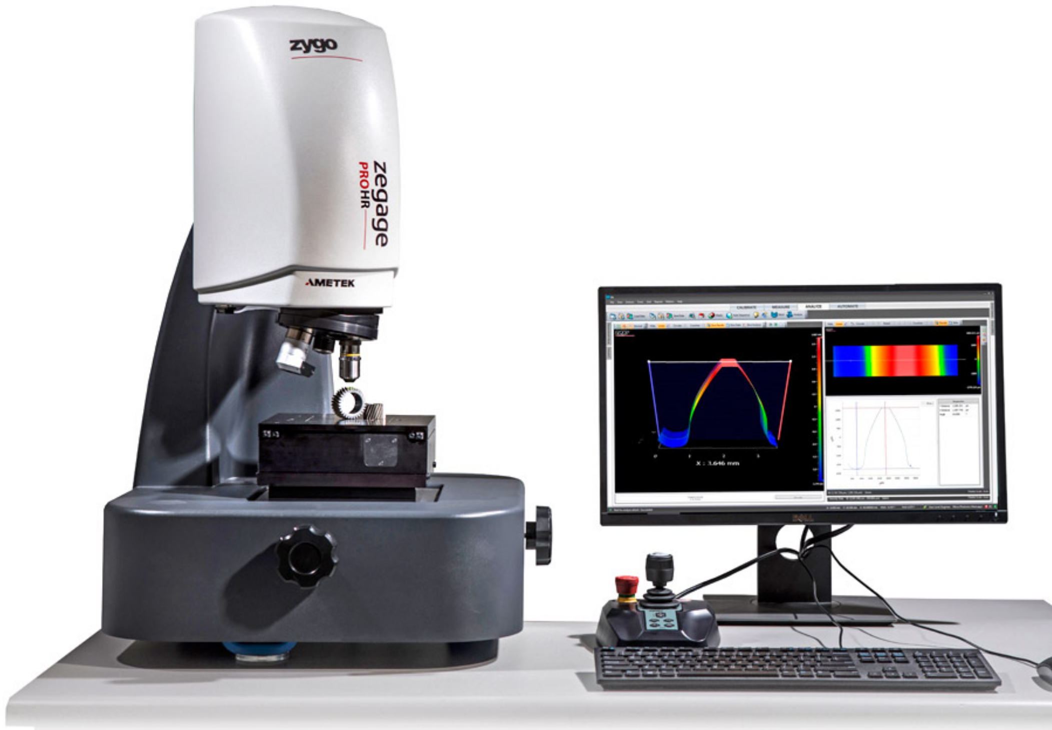

Principle of Optical profiling (white-Light Interferometry)

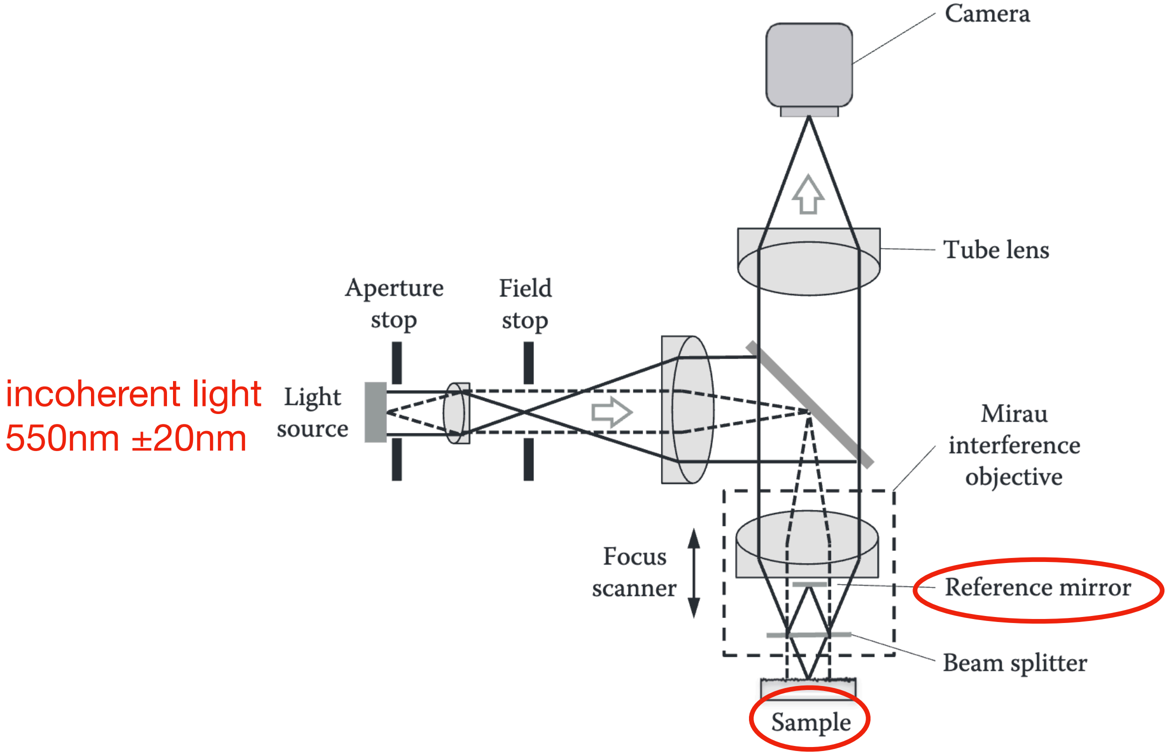

FIGURE 31.1 Interference microscope for areal surface structure analysis.

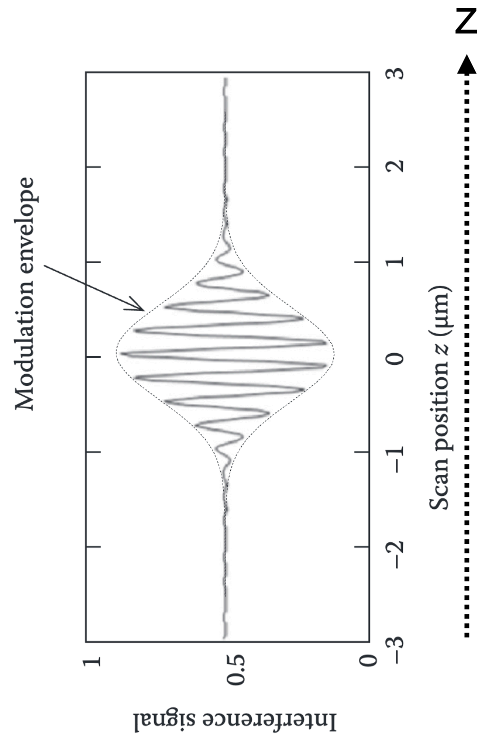

de Groot 2017

The instrument scans in z and—with AFM-level precision—assigns each pixel the height where the interference envelope between reference and sample reflections reaches its maximum.

2-D Interference Fringes Trace Surface Height Contours

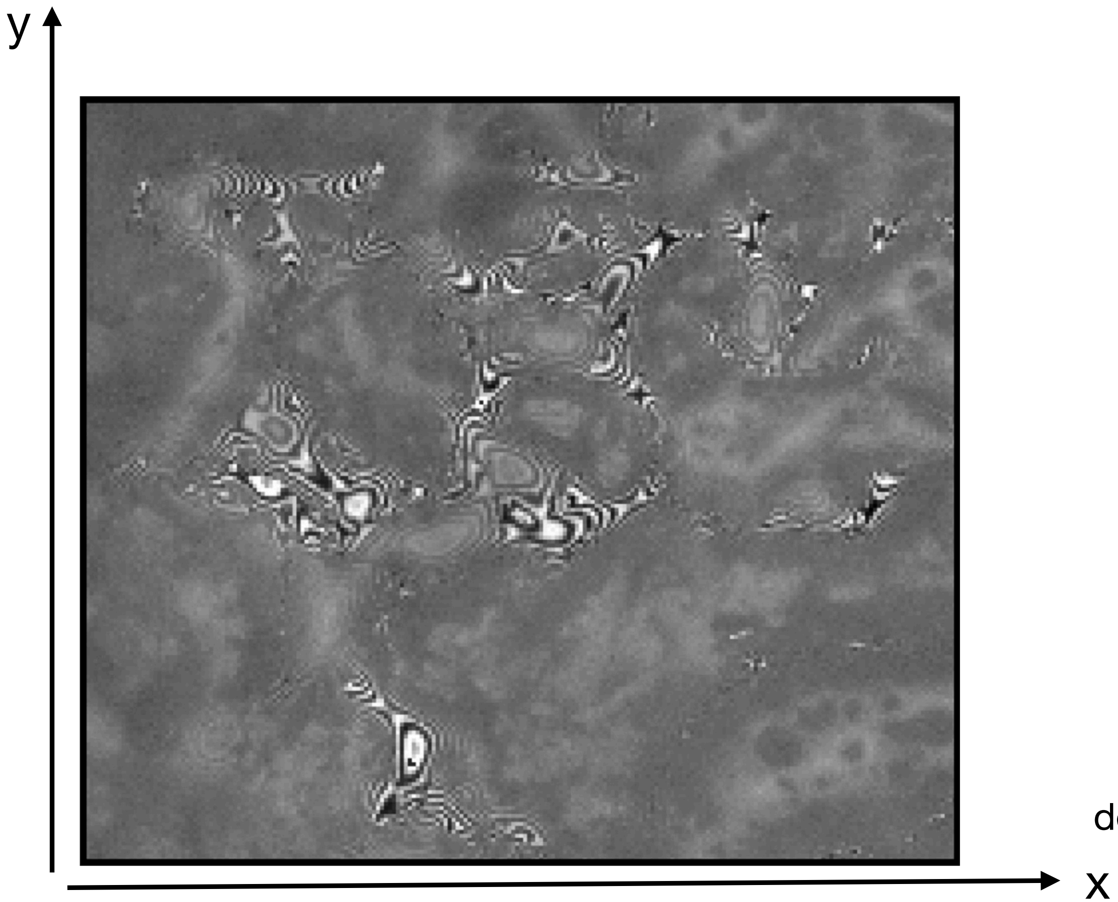

de Groot 2017

- Only points whose optical path matches the reference mirror appear as high-contrast fringes.
- The resulting contours indicate equal height.

Diffraction-Limited Resolution in Interference Fringe Imaging

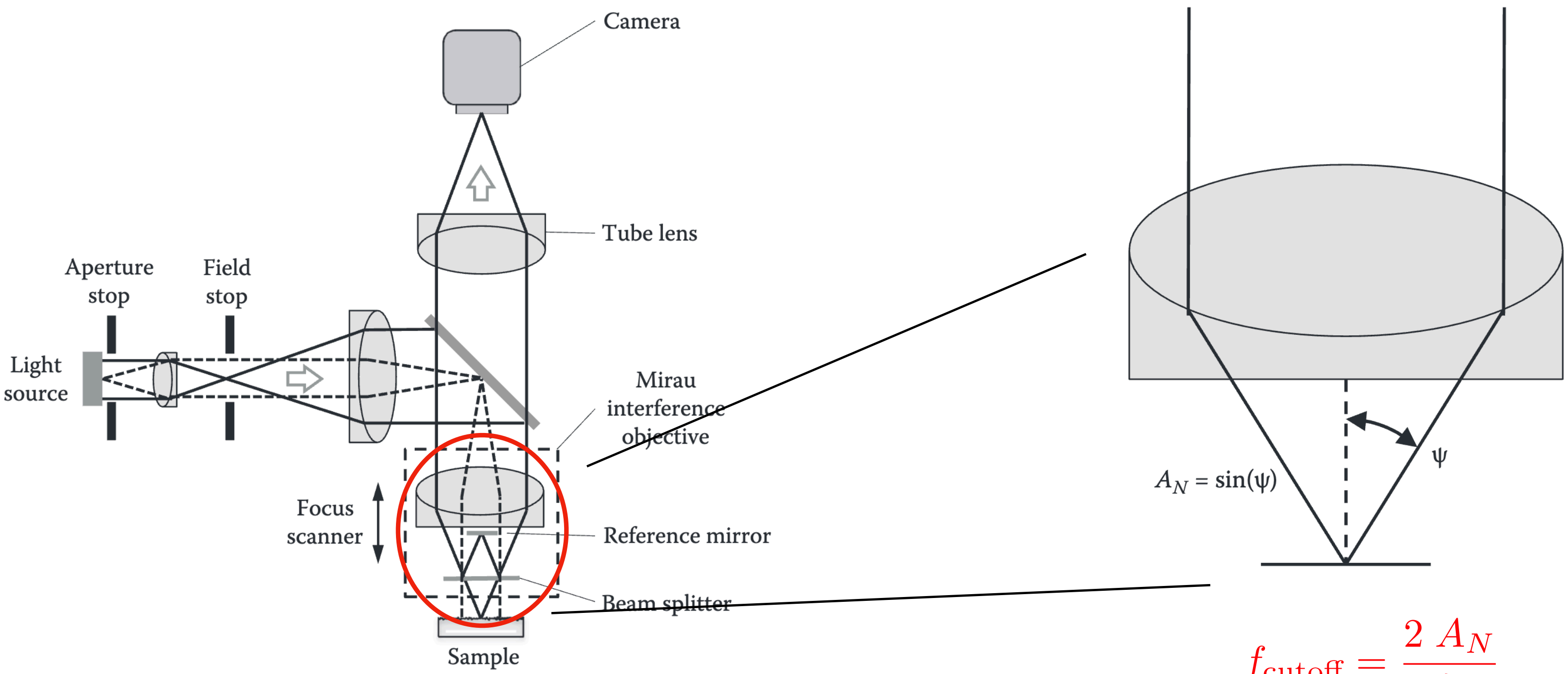

$$f_{\text{cutoff}} = \frac{2\ A_N}{\lambda}$$

The 2-D interference fringe pattern is diffraction-limited: spatial frequencies above the cutoff are suppressed, so the finest height details cannot be reproduced.

Diffraction-Limited Transfer in WLI Blurs Fine Surface Features

AFM

WLI
(raw data)

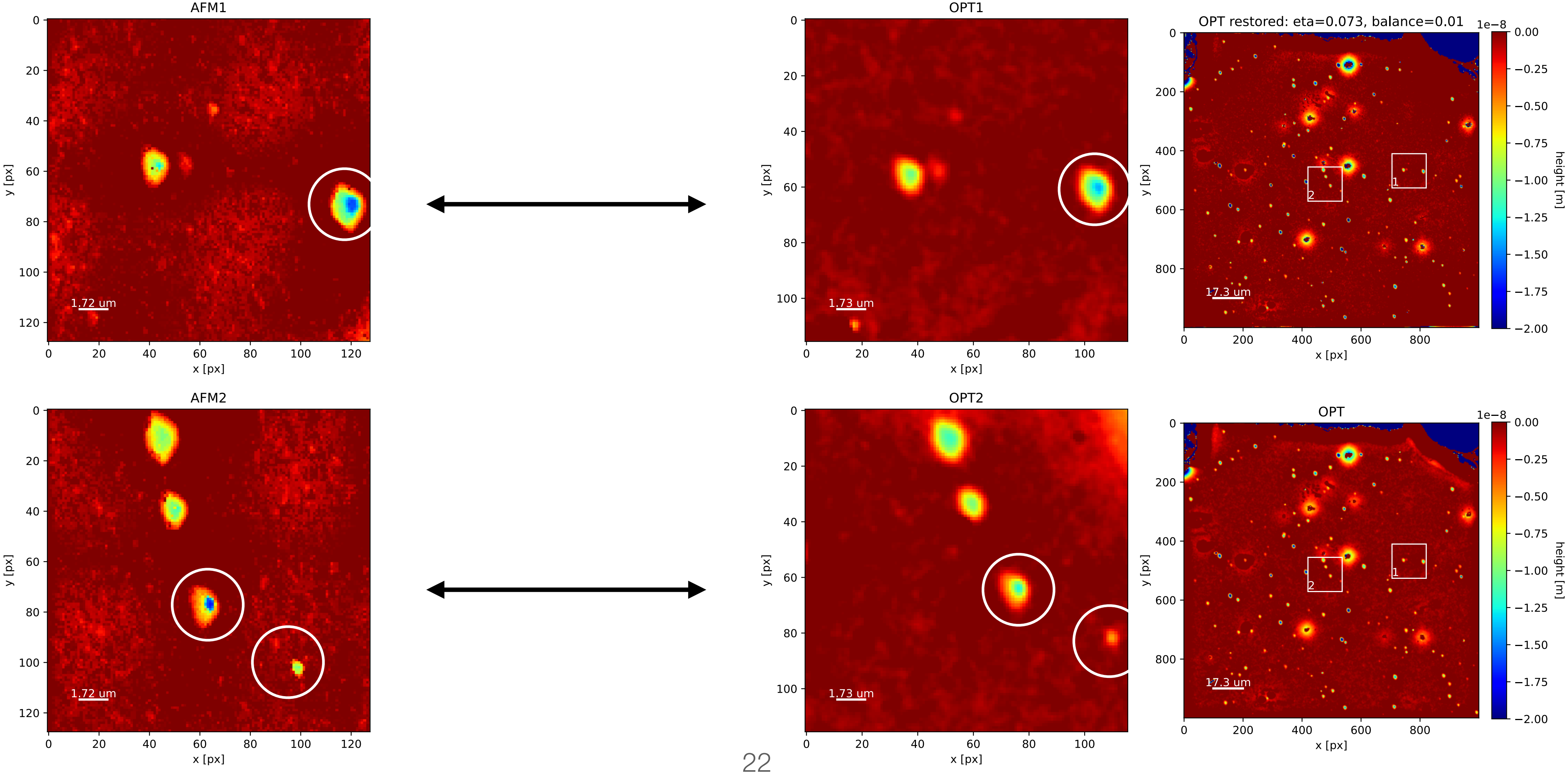

BPRA Quantifies the Diffraction-Limited Transfer Function

opticaopen.28614767

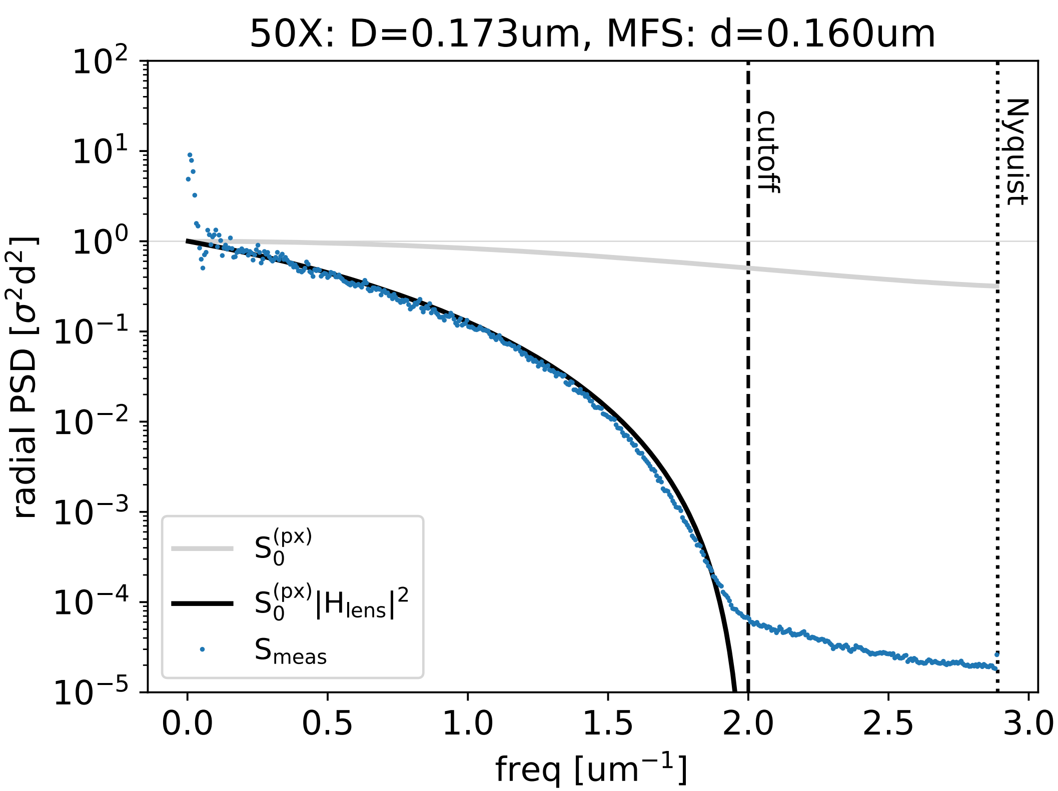

$$\mathcal{F}\left\{z[x,y]\right\} = H[f_x, f_y]\mathcal{F}\left\{z_0[x,y]\right\}$$

Fourier transform transfer function

Binary Pseudo-Random Array (BPRA)

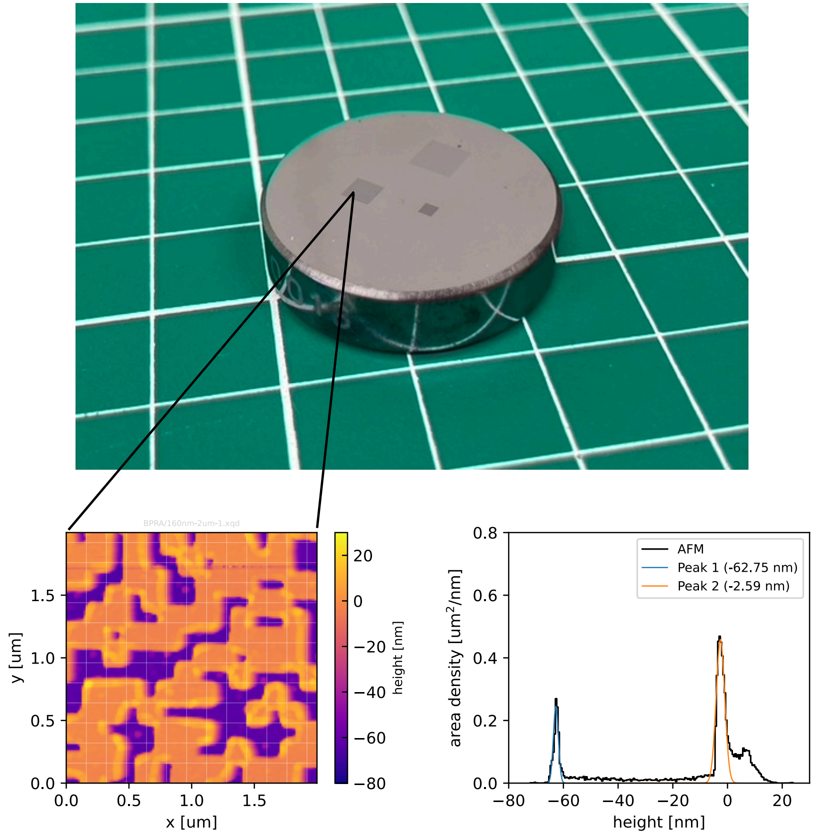

A two-level pixel pattern is randomly distributed across a two-dimensional plane.

Topography Restoration with the Measured Transfer Function

$$\mathcal{F}\left\{z_0[x,y]\right\} = \frac{1}{H[f_x,f_y]}\mathcal{F}\left\{z[x,y]\right\}$$

Measured topography

$z[x,y]$

FFT

Fourier spectrum

$\mathcal{F}\left\{z[x,y]\right\}$

restoration

Corrected Fourier spectrum

$\frac{1}{H[f_x,f_y]}\mathcal{F}\left\{z[x,y]\right\}$

inverse FFT

Restored topography

$\mathcal{F}^{-1}\left\{\frac{1}{H[f_x,f_y]}\mathcal{F}\left\{z[x,y]\right\}\right\}$

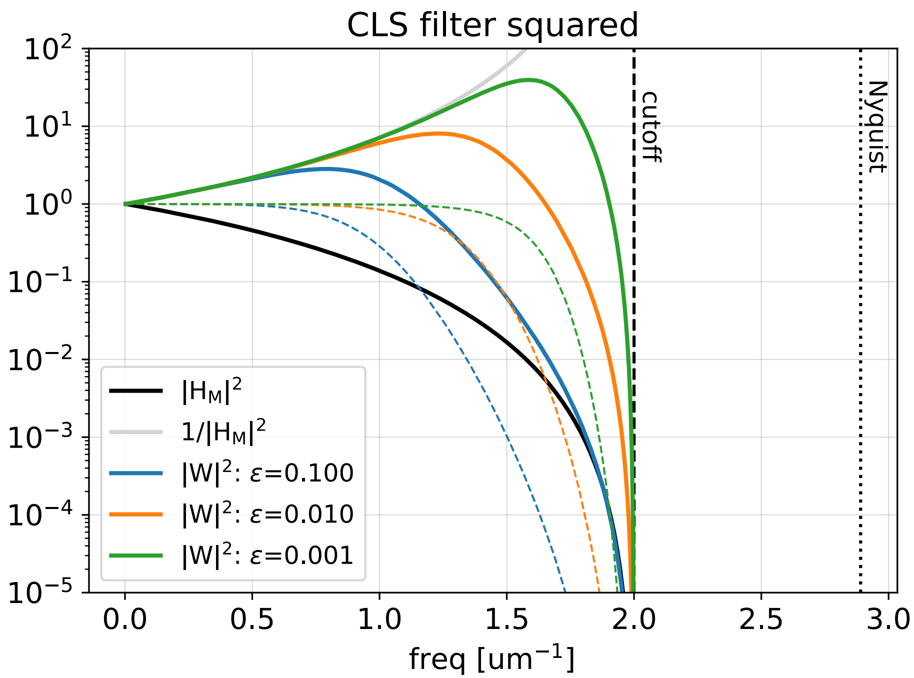

opticaopen.28614767

Restored WLI Topography Approaches AFM-Level Fine Detail

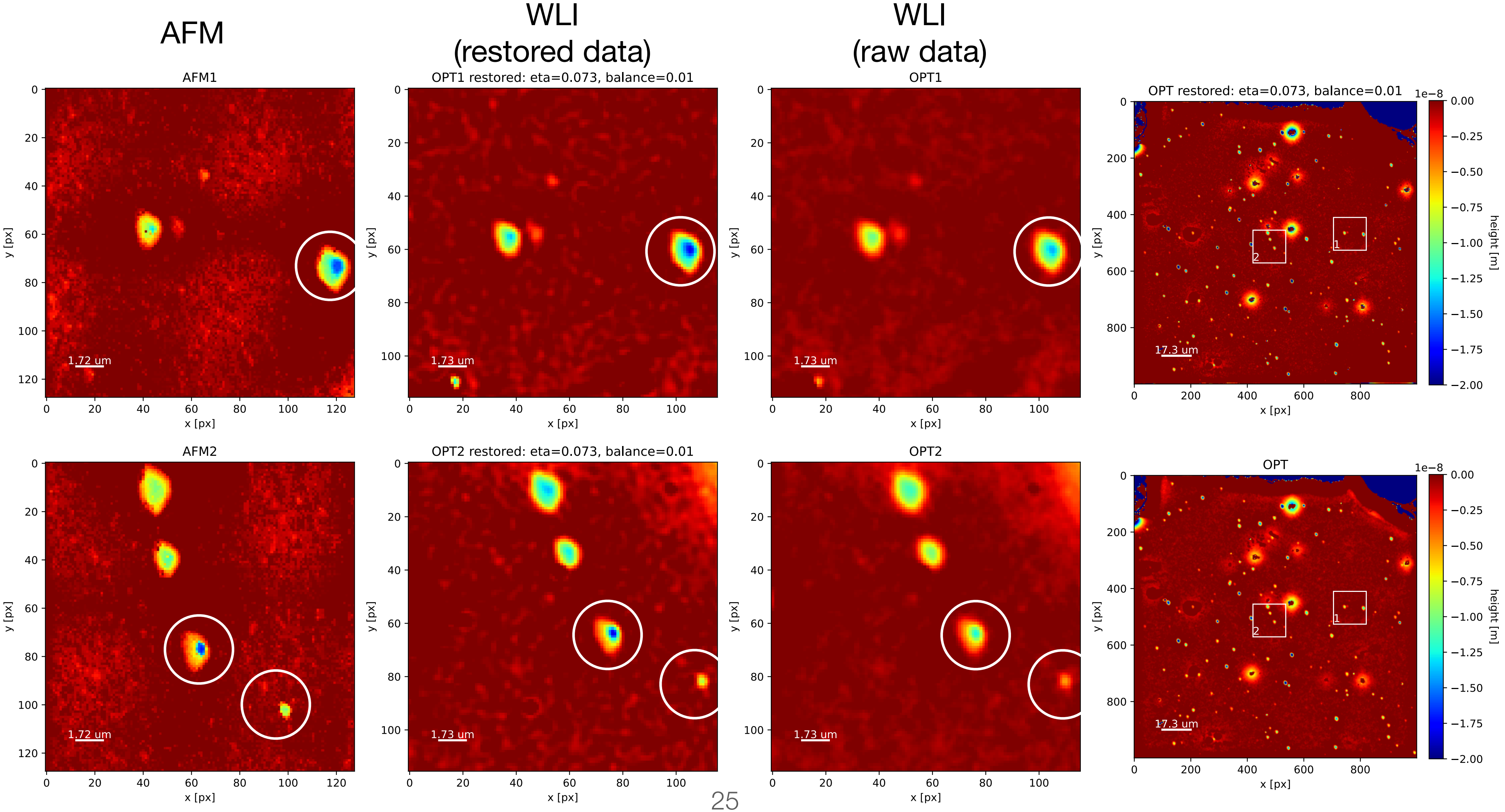

Impact of restoration on the pit-depth histogram

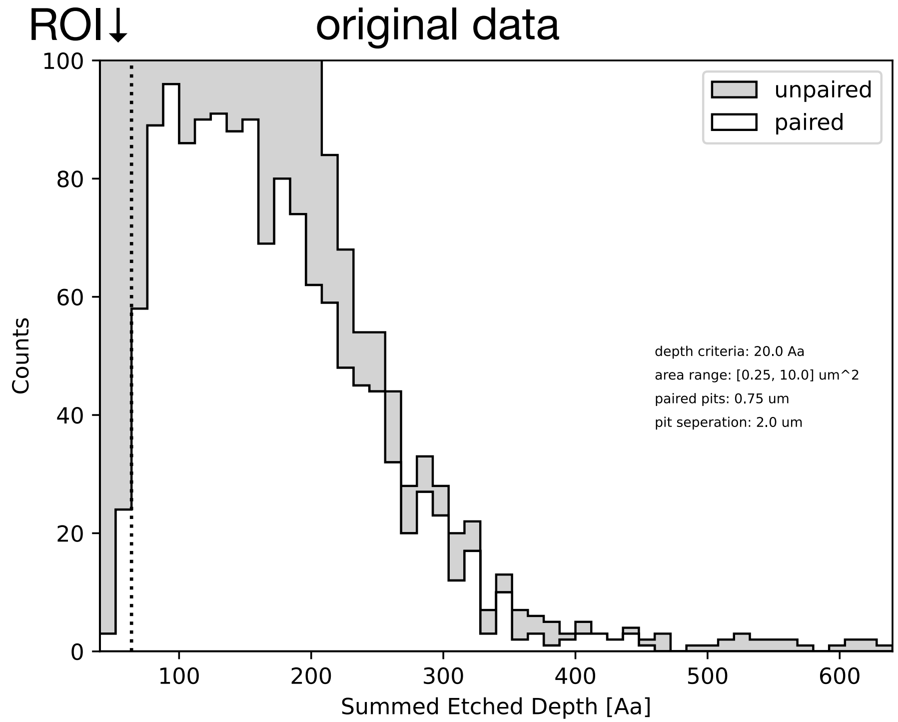

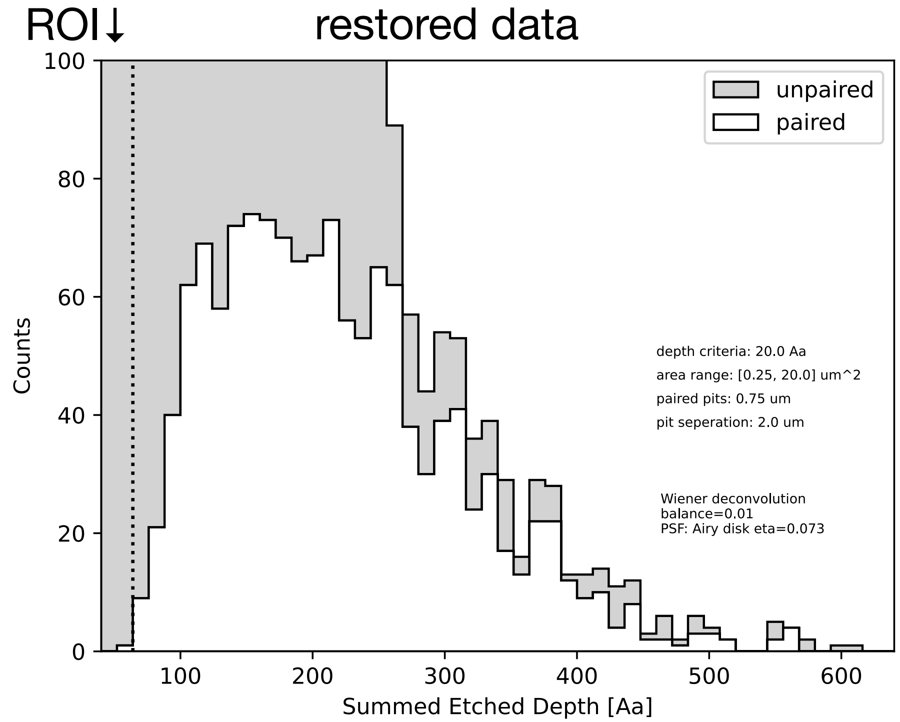

Restoration shifts α-recoil pits to larger depths, leaving the shallow-depth ROI almost empty.

3. Etch-pit formation model

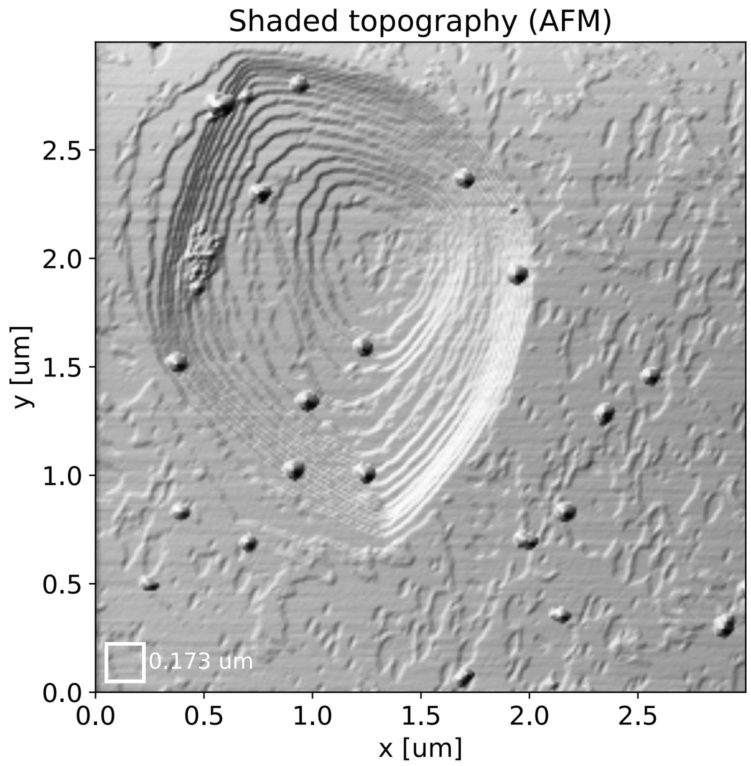

Recoil Energy – Track Length Correspondence

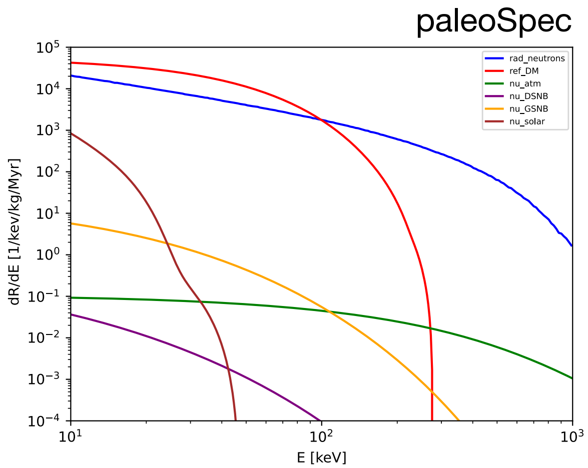

Recoil energy spectrum
(Theory)

Baum et al. 2020

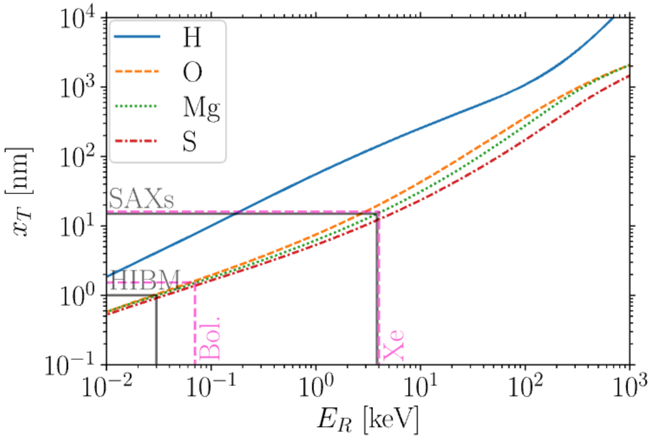

Recoil energy—track length relation
(SRIM table)

Drukier et al. 2019

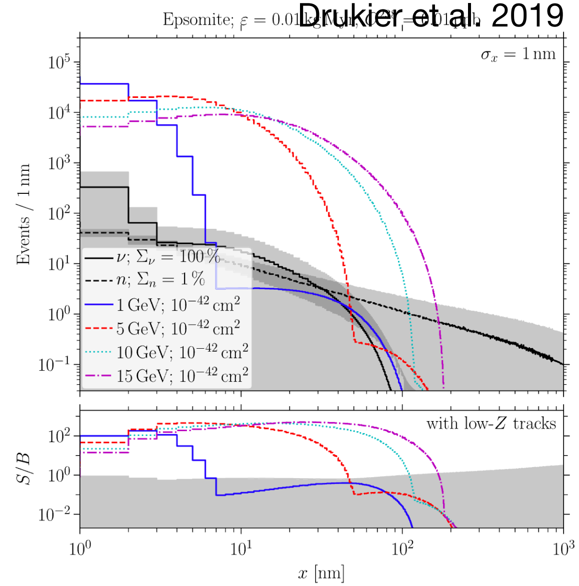

Track length histogram
(Observable)

SRIM tables convert recoil energy to track length, mapping the theoretical spectrum to the observed histogram—and the measured track-length distribution, in turn, reveals the recoil-energy spectrum.

Etch-Pit Yield vs. Stopping Power

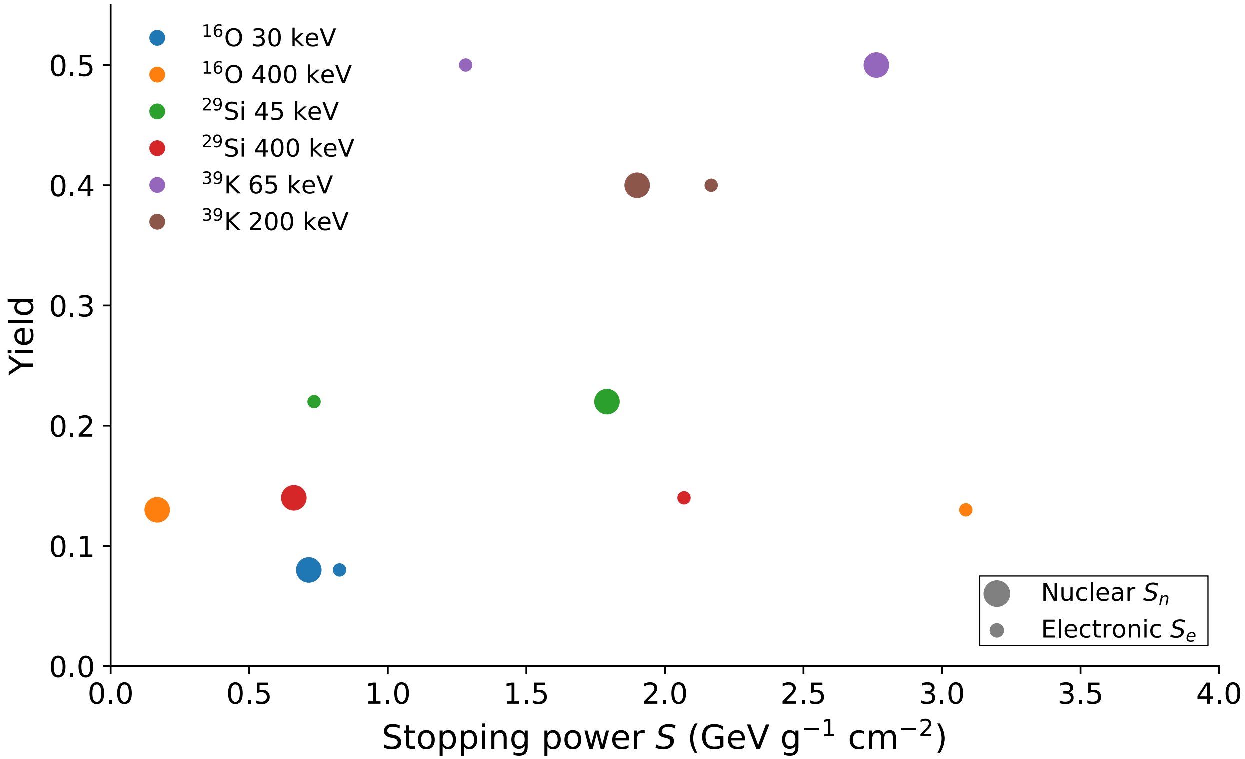

Based on Table 1 in Snowden-Ifft & Chan (1995)

Snowden-Ifft and Chan implanted ions into mica and showed that the etch-pit yield—pits per incident ion—depends mainly on the nuclear stopping power, with little sensitivity to the electronic component.

Unit-Layer Quantization of Etch-Pit Depths

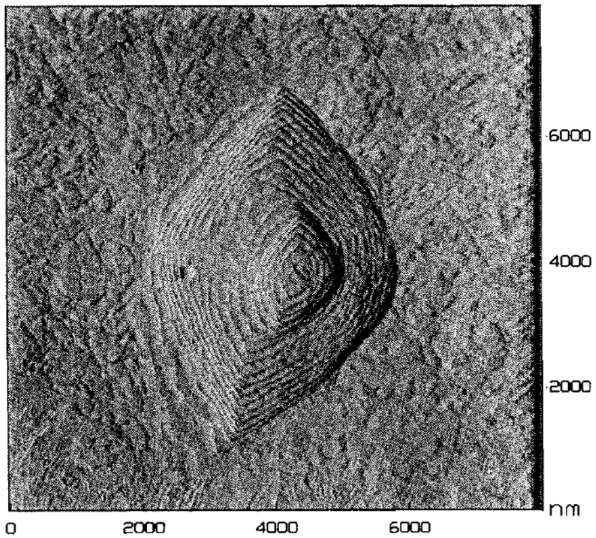

FIG. 1. Alpha-recoil track revealed by etching muscovite mica in 49% HF for 4 h. All such etch pits in the sample have the same symmetry: long axis oriented along the Y axis; shallower wall along the negative X axis with origin at the center of the etch pit; steeper wall along the positive X axis. Along Y the steps are 2 nm in height; along negative X the steps have split into pairs with 1-nm step heights. Along positive X they are too close together to resolve. The images in Figs. 1, 2, and 3 were taken in "constant height mode" with slight feedback gain to highlight the step edges. The step heights were determined by making a second scan, under "constant force mode."

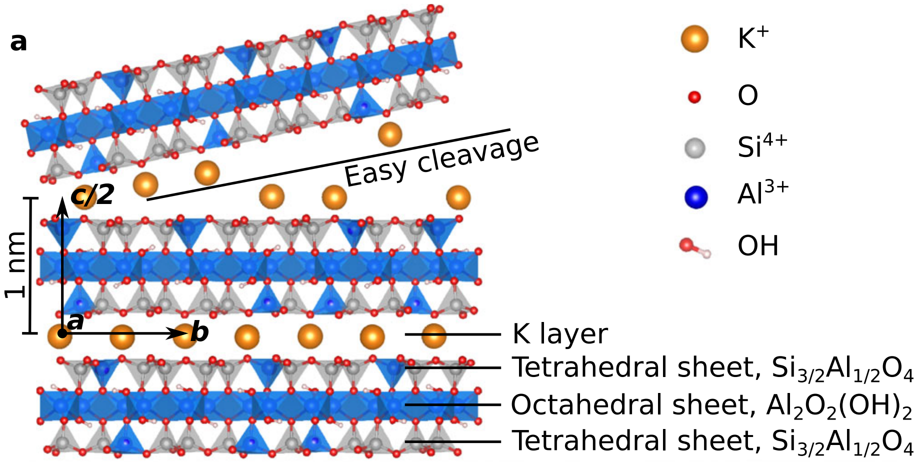

Snowden-Ifft et al. (1993)

Etching pits in muscovite mica advance in 1 nm increments—precisely the thickness of a single layer—so the measured pit depths occur only at integer-nanometre steps (Snowden-Ifft et al. 1993).

Phenomenological Model for the Energy—Depth Relation

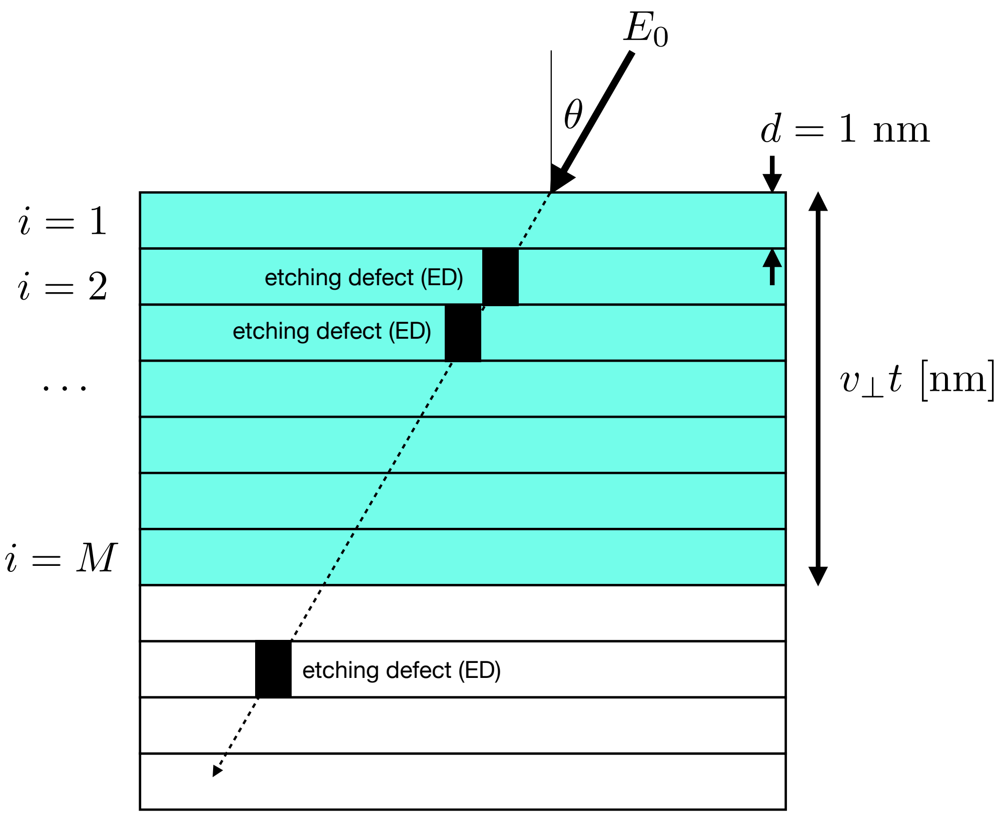

Recreated from Fig. 1 of Snowden-Ifft & Chan (1995)

- **Observed pit depth**

$$D = d \sum_{i=1}^{M} \chi_i$$

- **Probability of an etching defect in the i-th layer**

$$\Pr\left(\chi_i = 1 | E_i\right) = 1 - \exp\left(-\frac{k_e S_e(E_i) + k_n S_n(E_i)}{\cos\theta}\right)$$

- **Number of layers removed during etching**

$$M = \frac{v_\perp \, t}{d}$$

An ion stochastically creates EDs in each 1-nm-layer with probability Pr(χ_i = 1|E_i).
Pit depth equals the layer thickness multiplied by the number of ED-bearing layers removed.

Recoil Energy – Pit Depth Correspondence

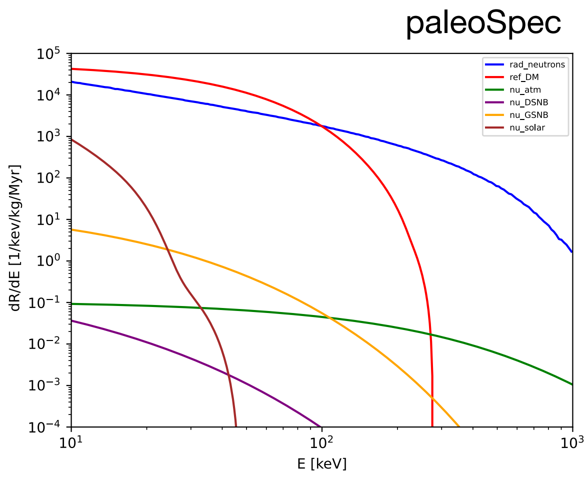

Recoil energy spectrum (Theory)

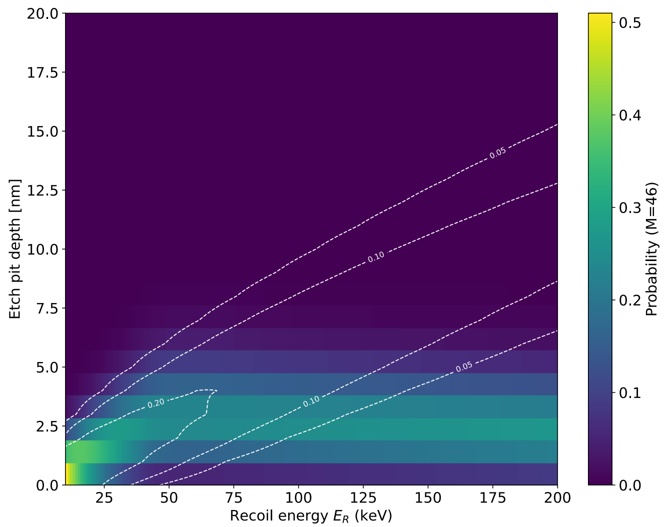

Recoil energy—pit depth relation (Snowden-Ifft and Chan 1995)

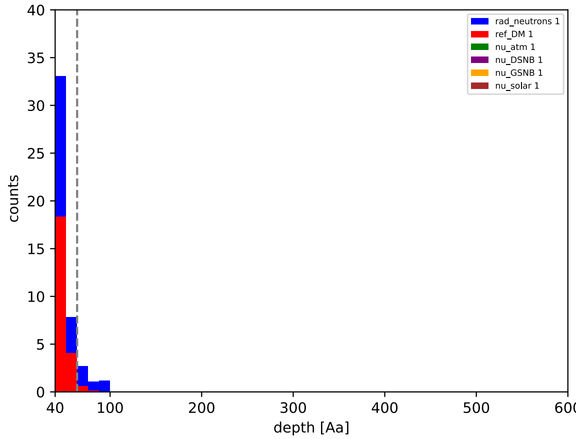

Pit depth histogram (Observable)

Etched tracks are observed as a pit-depth histogram. Snowden-Ifft & Chan (1995) convert recoil energy into pit depth, serving the same role for etched pits that SRIM plays for track lengths.

Measurement of Perpendicular Bulk Etch Rate, $v_{\perp}$

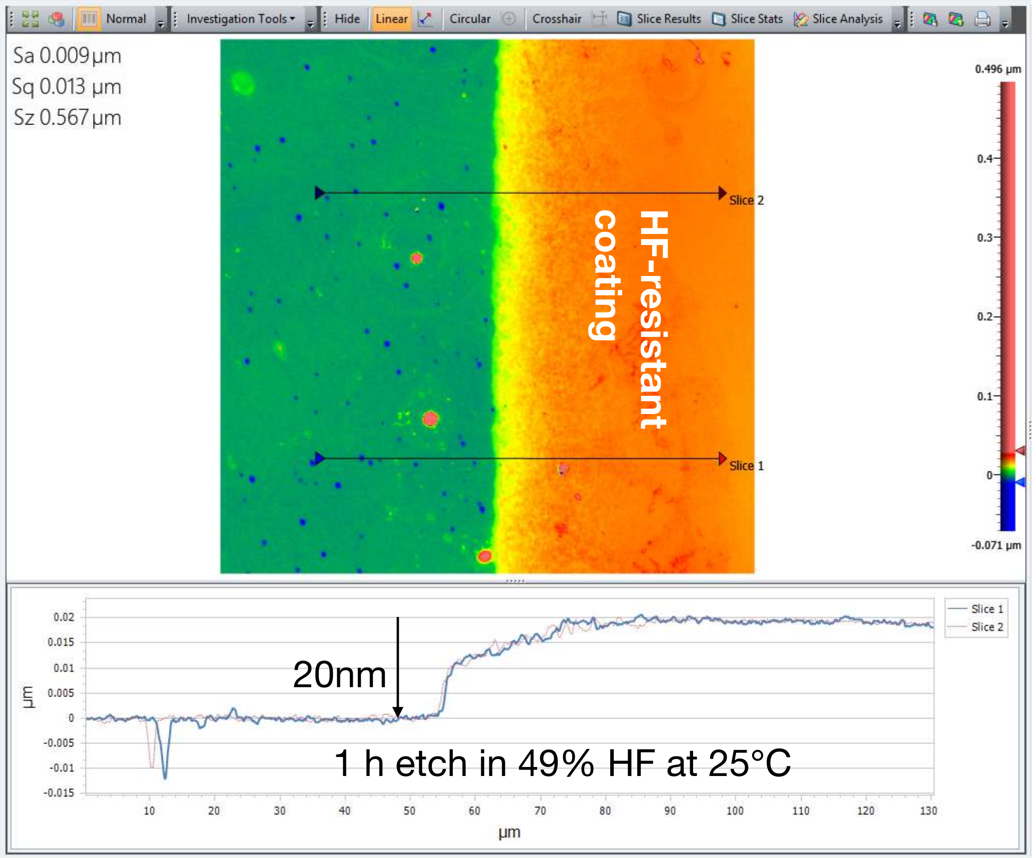

Dartyge et al. 1981	12 nm/h	fission-track intersections
Price and Salamon 1986	22 nm/h	surface density of α-recoil tracks
Freeman and Snowden-Ifft 1995	18, 20, 23 nm/h	laser interferometer
Hirose et al. (this study)	20 nm/h	HF-resistant coating

Summary for DMICA overview

- DMICA extends Snowden-Ifft's DM search with etched mica samples.
- Recoil tracks appear as nm-deep pits after chemical etching.
- Fast-neutron recoil pits demonstrate mica's capability as a DM detector.
- Pit depth is a key observable; its histogram separates dark-matter-like pits from α-recoil pits.
- DMICA targets an exposure of one ton-year in practical time by scanning mica with an optical profiler.
- A 0.5 mm^2 R&D scan reproduced Snowden-Ifft's pit-depth histogram.
- The extremely flat geometry of DMICA boosts the surface-to-volume ratio, giving reach to ultra-heavy DM at very low flux.